Analysis of Low-Temperature Intermetallic Growth in Copper-Tin Diffusion Couples

Z. MEI, A.J. SUNWOO, and J.W. MORRIS, Jr.

A multiphase diffusion model was constructed and used to analyze the growth of the ε- and η-phase intermetallic layers at a plane Cu-Sn interface in a semi-infinite diffusion couple. Experimental measurements of intermetallic layer growth were used to compute the interdiffusivities in the ε and η phases and the positions of the interfaces as a function of time. The results suggest that interdiffusion in the ε phase ($\tilde{D}_\varepsilon$) is well fit by an Arrhenius expression with $D_0 = 5.48 \times 10^{-9}$ m^2/s and $Q = 61.9$ kJ/mole, while that in the η phase ($\tilde{D}_\eta$) has $D_0 = 1.84 \times 10^{-9}$ m^2/s and $Q = 53.9$ kJ/mole. These values are in reasonable numerical agreement with previous results. The higher interdiffusivity in the η phase has the consequence that the η phase predominates in the intermetallic bilayer. However, the lower activation energy for interdiffusion in the η phase has the result that the ε phase fills an increasing fraction of the intermetallic layer at higher temperature: at 20 °C, the predicted ε-phase thickness is $\approx$10 pct of that of η, while at 200 °C, its thickness is 66 pct of that of η. In the absence of a strong Kirkendall effect, the original Cu-Sn interface is located within the η-phase layer after diffusion. It lies near the midpoint of the η-phase layer at higher temperature (220 °C) and, hence, appears to shift toward the Sn side of the couple. The results are compared to experimental observations on intermetallic growth at solder-Cu interfaces.

I. INTRODUCTION

TIN-bearing solders are widely used to join Cu leads in electronic devices and to protect Cu leads from oxidation during storage prior to assembly (pretinning). The solder bonds strongly to Cu because of the formation of Cu-Sn intermetallics at the wetted interface. However, the intermetallic layer can be a source of mechanical weakness in soldered joints due to brittle cracking of the intermetallic or delamination at the interface and may lead to loss of solderability through excessive growth during storage. Because of their importance to bonding and subsequent properties, many experimental studies have been done on Cu-Sn intermetallic phases and have treated their crystal structures[1] and morphologies,[2–14] their effects on mechanical properties[15,16,17] and solderability,[2–5,18,19] and changes in their structure or properties on the addition of other elements into either the copper or the tin-lead solder.[11,12,18]

The intermetallic layer at the solder-Cu interface thickens relatively rapidly during initial soldering or reflow, since the temperature is relatively high and the solder phase is molten. It continues to grow, though much more slowly, during storage and service. This growth in the solid state is of particular technological concern, since it occurs continuously and may cause delayed and unpredicted problems. While a number of empirical relations have been proposed to predict the intermetallic layer thickness as a function of time and temperature,[4,6,7,9,10,12,13] there is less theoretical work of the sort that can generate predictive analytic models. Part of the reason for this is the structural complexity of the wetted interface, which, in the common case of eutectic solder on copper, has a two-phase Pb-Sn solder separated from copper by an intermetallic bilayer with ε phase (Cu_3Sn) adjacent to the Cu and η phase (Cu_6Sn_5) next to the solder.

To simplify the problem, we follow Onishi and Fujibuchi[6] in considering interdiffusion at low temperature in a simple Cu-Sn couple and formulate an analytic solution for the planar growth of the intermetallic bilayer. While the results are only qualitatively applicable to intermetallic growth in the solder joint, they allow us to evaluate the interdiffusion coefficients in the intermetallic phases and help to explain important features of intermetallic growth in solder. These include the preponderance of the η-phase intermetallic in joints that thicken at relatively low temperature and the apparent shift of the original interface toward the Sn side during growth at higher temperature.

II. BACKGROUND

It will be useful to briefly review the relevant experimental observations before framing the analytical model. As expected from the Cu-Sn equilibrium phase diagram,[20] two intermetallic phases are observed at a Cu-Sn interface, ε (Cu_3Sn) and η (Cu_6Sn_5). (In fact, the hexagonal η phase undergoes a secondary ordering reaction into the long-period, η' phase at $\approx$180 °C; we shall ignore this transition, which does not appear to have an important effect on the Cu-Sn interdiffusivity.) The relative fractions of the two phases in the intermetallic layer depend on temperature. The intermetallic layer that forms on initial contact with molten solder is ordinarily η phase. However, if the molten solder has a temperature greater than 415 °C, the peritectic temperature of the η phase, the initial layer has the more stable ε structure. When a Cu-Sn or Cu-solder couple with an η-phase layer is aged

Z. MEI, Research Engineer, and J.W. MORRIS, Jr., Professor of Metallurgy, are with the Center for Advanced Materials, Lawrence Berkeley Laboratory, and the Department of Materials Science and Mineral Engineering, University of California, Berkeley, CA 94720. A.J. SUNWOO, Staff Scientist, is with the Lawrence Livermore National Laboratory, Livermore, CA 94550.

Manuscript submitted July 23, 1991.

at relatively low temperature (20 °C to 70 °C), it grows without developing an obvious ε layer.[1,5,7,9,10,14] When the system is aged at higher temperature (135 °C to 220 °C), both η and ε layers appear.[1,2–14]

The thickness (W) of the intermetallic layer can be represented by an equation of the usual form

$$W = W_0 + At^n \quad [1]$$

The exponent, n, is 0.5 for ordinary diffusional growth and has this value for intermetallic growth in a semi-infinite Cu-Sn couple.[6] However, thin solder layers have a lower value of the exponent, $n \approx 0.33$.[4,10]

It is reported that inert markers in a Cu-Sn diffusion couple are displaced toward the Cu side during growth at low temperature (20 °C to 70 °C)[14] but toward the Sn side at higher temperature (>170 °C).[6,21,22] These observations have been interpreted to mean that Cu diffusion dominates at low temperature, while Sn diffusion is dominant at higher temperature. The relatively rapid low-temperature diffusion of Cu in Sn, Pb, and Sn-Pb alloys is due to its interstitial diffusion mechanism.[23–26]

Most solders are Sn-Pb alloys. Although Pb does not form any intermetallic phases with Cu or Sn, it affects the growth rate of the Cu-Sn intermetallic layer.[19] A small addition of Pb into Sn reduces the intermetallic growth rate by reducing the Sn concentration at the interface. However, the growth rate increases again as the Pb content approaches 38 wt pct (the Pb-Sn eutectic point); diffusion in the eutectic is enhanced by the large interfacial area and the relatively low melting point. Because of these counterbalancing effects, the rate of intermetallic growth into solder is not that different from the rate of growth into pure Sn in a binary Cu-Sn diffusion couple.

III. ANALYTIC MODEL

A. *Assumptions*

We consider a binary diffusion couple of semi-infinite copper and tin plates that are brought into contact at $t = 0$. The two intermetallic phases, ε and η, form as layers and grow as planar plates (Figure 1), so that the net diffusion is one-dimensional. Four additional assumptions are used.

(1) The intrinsic diffusion coefficients D_{Cu} and D_{Sn}, are constant within each individual phase. This assumption seems reasonable since the η and ε intermetallics have narrow composition ranges, and there is little mutual solubility of Cu and Sn at temperatures below 200 °C.

(2) Kirkendall voids have a negligible effect. Since the intrinsic diffusivities of Cu and Sn in the terminal solid solutions are different (Reference 36 or Table I), Kirkendall voids may form in the joint. While voids are observed in constrained, high-temperature Cu-Sn diffusion couples of the sort formed, for example, in the processing of "internal tin" superconducting wire[27] and voids are occasionally found at the solder-intermetallic interface in solder joints,[28] the volume fraction of voids observed in solder joints and diffusion couples treated at low temperature is small enough that its effect on the intermetallic growth rate should be negligible. In the absence of Kirkendall voiding, diffusion is governed by the Darken interdiffusion coefficient[29] that includes the lattice movement induced by the vacancy wind:

$$\tilde{D}_{Cu} = \tilde{D}_{Sn} = \frac{C_{Cu}}{C_{Cu} + C_{Sn}} D_{Sn} + \frac{C_{Sn}}{C_{Cu} + C_{Sn}} D_{Cu} \quad [2]$$

By using the interdiffusion coefficients, only the effective interdiffusion of copper needs to be considered; the interdiffusion of tin is equal and opposite.

(3) The volume change on forming the intermetallic is neglected. There is, in fact, a significant decrease in volume when either of the intermetallic phases forms. Measured lattice parameter data[30,31,32] show a net 8.2 pct decrease in volume when pure Cu and Sn combine into Cu_3Sn (ε) and a net 10 pct decrease when they form Cu_6Sn_5 (η). However, even a 10 pct volume decrease translates into only a 3 pct decrease in the linear growth rate of a relaxed planar layer, which is within the accuracy of measurement of the growth of intermetallic layers in practice.

(4) Chemical equilibrium is assumed at the growing interfaces. This assumption is supported by the electron microprobe measurements of Onishi and Fujibuchi[6] for the particular case of the Cu-Sn diffusion couple. The ε phase appears somewhat difficult to nucleate and is not observed in thin intermetallic layers that are predominantly η.[5] However, the ε phase is found under conditions in which the analysis that follows predicts that it should have a significant thickness in the intermetallic layer.

B. *Basic Equations*

The problem presented in Figure 1 is that of binary element, multiphase diffusion. A solution to the diffusion equation for a binary element, two-phase system was proposed by Wagner and is given by Jost.[33] This solution was extended to multiphase systems by Kirkaldy.[34] The solution we shall use is a special case

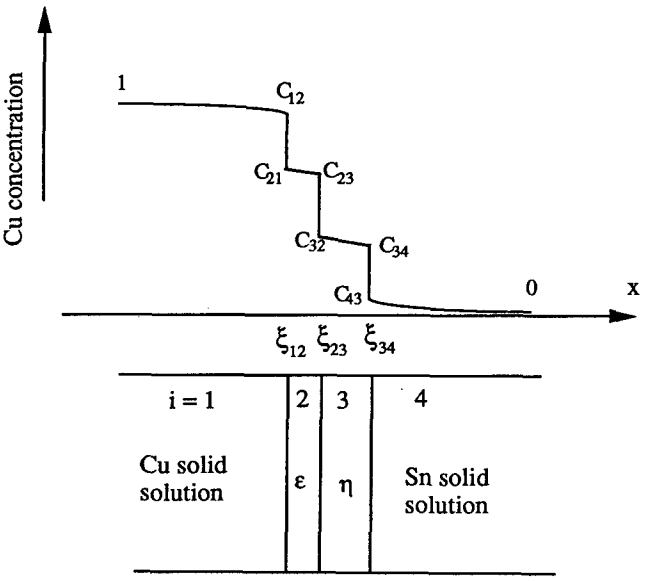

Fig. 1 — Schematic drawing of the analytical model.

Table I. Diffusion Coefficients

Type of Diffusion	Q (kJ/mol)	D_0 (m^2/s)	D (at 20 °C)	D (at 190 °C)	D (at 200 °C)	D (at 210 °C)	D (at 220 °C)	Reference
$D_{Cu\text{-in-}Cu}$	195.6	3.4×10^{-5}	4.40×10^{-40}	2.82×10^{-27}	8.26×10^{-27}	2.31×10^{-26}	6.22×10^{-26}	36
$D_{Sn\text{-in-}Sn}$	43.89	1.2×10^{-9}	1.78×10^{-17}	1.33×10^{-14}	1.70×10^{-14}	2.14×10^{-14}	2.67×10^{-14}	36
$D_{Cu\text{-in-}Sn}$	33.02	2.4×10^{-7}	3.09×10^{-13}	4.49×10^{-11}	5.39×10^{-11}	6.41×10^{-11}	7.57×10^{-11}	23
$D_{Sn\text{-in-}Cu}$	177.0	2.95×10^{-5}	4.67×10^{-34}	3.10×10^{-25}	8.19×10^{-25}	2.08×10^{-24}	5.09×10^{-24}	22
$\tilde{D}_{Cu}$	—	—	4.65×10^{-34}	3.08×10^{-25}	8.13×10^{-25}	2.07×10^{-24}	5.07×10^{-24}	comp. from intrinsic diffusivity
$\tilde{D}_{Sn}$	—	—	3.09×10^{-13}	4.49×10^{-11}	5.39×10^{-11}	6.41×10^{-11}	7.56×10^{-11}	

of Kirkaldy's and is briefly derived below. The symbols are defined in the appended List of Symbols.

The copper concentration in phase i, C_i, (i = 1 through 4: Cu solid solution, ε, η, and Sn solid solution, respectively) satisfies Fick's Second Law and, hence, has the form

$$C_i = A_i - B_i \operatorname{erf}\left(\frac{x}{2\sqrt{\tilde{D}_i t}}\right) \quad (i = 1 \text{ through } 4) \quad [3]$$

where erf (x) is the error function and A_i and B_i are constants to be determined from the boundary conditions.

Assuming local equilibrium at the interfaces and letting ξ_{ij} be the instantaneous position of the (ij) interface, C_{ij} the concentration on the i side of the interface, and C_{ji} the concentration on the j side, the boundary conditions are

$$\begin{aligned} &C_1 = 1 \quad \text{at } x = -\infty \quad C_1 = C_{12} \quad \text{at } x = \xi_{12} \\ &C_2 = C_{21} \quad \text{at } x = \xi_{12} \quad C_2 = C_{23} \quad \text{at } x = \xi_{23} \\ &C_3 = C_{32} \quad \text{at } x = \xi_{23} \quad C_3 = C_{34} \quad \text{at } x = \xi_{34} \\ &C_4 = C_{43} \quad \text{at } x = \xi_{34} \quad C_4 = 0 \quad \text{at } x = \infty \end{aligned} \quad [4]$$

Mass conservation at the interface, ξ_{ij}, requires that

$$-\tilde{D}_i \frac{\partial C_i}{\partial x} + \tilde{D}_j \frac{\partial C_j}{\partial x} = (C_{ij} - C_{ji}) \frac{d\xi_{ij}}{dt} \quad (i = 1 \text{ through } 3, j = i + 1) \quad [5]$$

If the position of the (ij) interface changes as time as $\sqrt{t}$, then the function ξ_{ij} can be written

$$\xi_{ij} = 2\gamma_i \sqrt{\tilde{D}_i t} \quad (i = 1 \text{ through } 3) \quad [6]$$

where the γ_i are constants. Given these relations, the concentrations, C_i, satisfy both Eqs. [3] and [4] if

$$C_1 = 1 - \frac{1 - C_{12}}{1 + \operatorname{erf}(\gamma_1)} \left\{1 + \operatorname{erf}\left[\frac{x}{2\sqrt{\tilde{D}_1 t}}\right]\right\} \quad [7]$$

$$C_2 = C_{21} - \frac{C_{21} - C_{23}}{\operatorname{erf}(\gamma_2) - \operatorname{erf}(\gamma_1\sqrt{R_{12}})} \cdot \left\{\operatorname{erf}\left[\frac{x}{2\sqrt{\tilde{D}_2 t}}\right] - \operatorname{erf}[\gamma_1\sqrt{R_{12}}]\right\} \quad [8]$$

$$C_3 = C_{32} - \frac{C_{32} - C_{34}}{\operatorname{erf}(\gamma_3) - \operatorname{erf}(\gamma_2\sqrt{R_{23}})} \cdot \left\{\operatorname{erf}\left[\frac{x}{2\sqrt{\tilde{D}_3 t}}\right] - \operatorname{erf}[\gamma_2\sqrt{R_{23}}]\right\} \quad [9]$$

$$C_4 = \frac{C_{43}}{1 - \operatorname{erf}(\gamma_3\sqrt{R_{34}})} \left\{1 - \operatorname{erf}\left[\frac{x}{2\sqrt{\tilde{D}_4 t}}\right]\right\} \quad [10]$$

where $R_{ij} = \tilde{D}_i/\tilde{D}_j$. The unknowns, γ_i (i = 1 through 3), can be found by inserting Eqs. [7] through [10] into Eq. [5]. The results are

$$\frac{(1 - C_{12}) \exp(-\gamma_1^2)}{1 + \operatorname{erf}(\gamma_1)} - \frac{(C_{21} - C_{23}) \exp[-\gamma_1^2 R_{12}]}{\sqrt{R_{12}}[\operatorname{erf}(\gamma_2) - \operatorname{erf}(\gamma_1\sqrt{R_{12}})]} = (C_{12} - C_{21})\sqrt{\pi}\,\gamma_1 \quad [11]$$

$$\frac{(C_{21} - C_{23}) \exp(-\gamma_2^2)}{\operatorname{erf}(\gamma_2) - \operatorname{erf}[\gamma_1\sqrt{R_{12}}]} - \frac{(C_{32} - C_{34}) \exp[-\gamma_2^2 R_{23}]}{\sqrt{R_{23}}[\operatorname{erf}(\gamma_3) - \operatorname{erf}(\gamma_2\sqrt{R_{23}})]} = (C_{23} - C_{32})\sqrt{\pi}\,\gamma_2 \quad [12]$$

$$\frac{(C_{32} - C_{34}) \exp(-\gamma_3^2)}{\operatorname{erf}(\gamma_3) - \operatorname{erf}[\gamma_2\sqrt{R_{23}}]} - \frac{C_{43} \exp[-\gamma_3^2 R_{34}]}{\sqrt{R_{34}}[1 - \operatorname{erf}(\gamma_3\sqrt{R_{34}})]} = (C_{34} - C_{43})\sqrt{\pi}\,\gamma_3 \quad [13]$$

The equations listed above indicate that the interfacial position parameters, γ_i (i = 1 through 3), are determined by the ratios of the interdiffusion coefficients, $R_{ij} = \tilde{D}_i/\tilde{D}_j$ (i = 1 through 3, $j = i + 1$), rather than the interdiffusion coefficients themselves, $\tilde{D}_i$ (i = 1 through 4). This is because the movement of an interfacial position, according to Eq. [5], is to maintain the interfacial chemical equilibrium that is constantly unbalanced by the different chemical fluxes into and out of the interface. An interface (ij) could remain at the same position when $\tilde{D}_i$ (flux into the interface) increases, as long as $\tilde{D}_j$ (flux out the interface) increases also by a corresponding amount.

Equations [11] through [13] can be used in at least two ways. First, there are seven unknown parameters ($\tilde{D}_1$, $\tilde{D}_2$, $\tilde{D}_3$, $\tilde{D}_4$, γ_1, γ_2, γ_3) in three equations of Eqs. [11] through [13]. If the values of the interdiffusion coefficients, $\tilde{D}_i$ (i = 1 through 4), are provided, then the constants γ_i (i = 1 through 3) can be calculated from Eqs. [11] through [13]. Given the γ_i, the interfacial positions, and hence, the thicknesses of the intermetallic phases, can be found as functions of times from Eq. [6], and the composition profiles can be determined from Eqs. [7] through [10]. Second, if the interdiffusion coefficients are only known in the terminal Cu- and Sn-rich solutions ($\tilde{D}_1$ and $\tilde{D}_4$), then the interdiffusion coefficients in ε and η ($\tilde{D}_2$ and $\tilde{D}_3$) can be computed from experimental data on the layer thickness W *vs* time t. Since

$$\begin{aligned} W_\varepsilon &= k_\varepsilon\sqrt{t} = \xi_{2/3} - \xi_{1/2} \\ &= 2[\gamma_2\sqrt{\tilde{D}_2 t} - \gamma_1\sqrt{\tilde{D}_1 t}] \\ W_\eta &= k_\eta\sqrt{t} = \xi_{3/4} - \xi_{2/3} \\ &= 2[\gamma_3\sqrt{\tilde{D}_3 t} - \gamma_2\sqrt{\tilde{D}_2 t}] \end{aligned} \qquad [14a]$$

we have

$$\begin{aligned} k_\varepsilon &= 2[\gamma_2\sqrt{\tilde{D}_2} - \gamma_1\sqrt{\tilde{D}_1}] \\ k_\eta &= 2[\gamma_3\sqrt{\tilde{D}_3} - \gamma_2\sqrt{\tilde{D}_2}] \end{aligned} \qquad [14b]$$

There are only five unknown ($\tilde{D}_2$, $\tilde{D}_3$, γ_1, γ_2, and γ_3) in five equations (Eqs. [11] through [13] and [14b]).

C. *Numerical Calculations*

Numerical calculation is necessary to solve either of the problems described above since Eqs. [11] through [13] cannot be solved analytically for $\tilde{D}_i$ (i = 1 through 4) or γ_i (i = 1 through 3). The method adopted in this study is the Gauss-Newton method.[35]

The interdiffusion coefficients, $\tilde{D}_i$, are either known, or the unknown $\tilde{D}_i$ can be expressed in terms of the growth coefficients through Eqs. [14b]. In either case Eqs. [11] through [13] become three equations for the three unknowns, γ_i. To solve them by iteration, we define three new functions, $F_1(\gamma_1, \gamma_2, \gamma_3)$, $F_2(\gamma_1, \gamma_2, \gamma_3)$, and $F_3(\gamma_1, \gamma_2, \gamma_3)$, by setting $F_1(\gamma_1, \gamma_2, \gamma_3)$ equal to the difference between the left- and right-hand sides of Eq. [11] and defining $F_2(\gamma_1, \gamma_2, \gamma_3)$ and $F_3(\gamma_1, \gamma_2, \gamma_3)$ from the corresponding differences in Eqs. [12] and [13]. Denoting the values of γ_i (i = 1 through 3) that satisfy Eqs. [11] through [13] as γ_i^*,

$$F_j(\gamma_1^*, \gamma_2^*, \gamma_3^*) = 0 \quad (j = 1 \text{ through } 3) \qquad [15]$$

The coefficients γ_i^* are found by iteration. Given initial values, γ_i^0, that are in the neighborhood of the γ_i^*, first-order Taylor expansions of the F about the values, γ_i^0 (i = 1 through 3) give

$$\begin{aligned} F_j(\gamma_1^*, \gamma_2^*, \gamma_3^*) = F_j(\gamma_1^0, \gamma_2^0, \gamma_3^0) &+ \frac{\partial F_j}{\partial \gamma_1}\Delta\gamma_1 \\ &+ \frac{\partial F_j}{\partial \gamma_2}\Delta\gamma_2 + \frac{\partial F_j}{\partial \gamma_3}\Delta\gamma_3 \\ &(j = 1 \text{ through } 3) \end{aligned} \qquad [16]$$

where $\Delta\gamma_i = [\gamma_i^* - \gamma_i^0]$.

Rewriting Eq. [16] in a matrix format and making use of Eq. [15] gives

$$\begin{bmatrix} \frac{\partial F_1}{\partial \gamma_1} & \frac{\partial F_1}{\partial \gamma_2} & \frac{\partial F_1}{\partial \gamma_3} \\ \frac{\partial F_2}{\partial \gamma_1} & \frac{\partial F_2}{\partial \gamma_2} & \frac{\partial F_2}{\partial \gamma_3} \\ \frac{\partial F_3}{\partial \gamma_1} & \frac{\partial F_3}{\partial \gamma_2} & \frac{\partial F_3}{\partial \gamma_3} \end{bmatrix} \begin{bmatrix} \Delta\gamma_1 \\ \Delta\gamma_2 \\ \Delta\gamma_3 \end{bmatrix} = \begin{bmatrix} -F_1 \\ -F_2 \\ -F_3 \end{bmatrix} \qquad [17]$$

If the determinant of the matrix on the left side of Eq. [17] is not equal to zero, $\Delta\gamma_i$ can be found uniquely. Once they are found, the numbers γ_i^0 are replaced by the new numbers $[\gamma_i^0 + \Delta\gamma_i]$ and the process is repeated until the deviations, $\Delta\gamma_i$, become as small as desired. In the authors' experience, the calculation converges after about 20 iterations and is easily done on a desk-top computer.

The method suggested here can be contrasted with that suggested by Heumann[36,37] which was previously used by Onishi and Fujibuchi[6] to estimate the interdiffusivities of the ε and η phases. Heumann begins from an equation that is essentially identical to Eq. [5], which he derives from the Matano interface. This method requires values for the concentration gradients at the interface to calculate D_2 and D_3. Heumann suggested a linear approximation to simplify the calculation of $\partial C_i/\partial x$ (i = 1 through 4). The approximation is reasonable within the intermetallic phases, $\partial C_i/\partial x$ (i = 2 or 3), but is poor for the terminal solid solutions, $\partial C_i/\partial x$ (i = 1 or 4). The values of $\partial C_i/\partial x$ (i = 2 or 3) can be estimated from the interfacial equilibrium concentrations $C_{i,i-1}$ and $C_{i,i+1}$, and the intermetallic thickness; while the values of $\partial C_i/\partial x$ (i = 1 or 4) are difficult to approximate. Onishi and Fujibuchi[6] overcame the difficulty by measuring the concentration profiles with an electron probe microanalyzer.

The method developed in the previous section can be used to calculate the interdiffusion coefficients in the interfacial phases without resorting to either the linear gradient approximation or the careful concentration measurement. In the present case, the two methods yield very similar results.

IV. RESULTS AND DISCUSSION

We apply this method to compute the interdiffusion coefficients, $\tilde{D}_2 = \tilde{D}_\varepsilon$ and $\tilde{D}_3 = \tilde{D}_\eta$, from intermetallic data on the Sn-Cu diffusion couple measured by Onishi and Fujibuchi[6] and to study the rate and nature of intermetallic growth as a function of temperature.

A. *Diffusion Coefficients in Cu and Sn*

We first require the interdiffusion coefficient in the Cu and Sn terminal solid solutions. The interdiffusion coefficient in the ith phase is related to the intrinsic diffusivities in that phase according to Eq. [2]. The intrinsic diffusivities in Cu and Sn solid solutions have previously been measured[22,23,36] and set in the Arrhenius form:

$$D = D_0 \exp\left[-\frac{Q}{RT}\right] \qquad [18]$$

The experimental values of D_0 and Q depend on the concentration values in the solid solutions. Since the solubilities of the terminal solutions are small over the temperature range of interest (<220 °C), the interdiffusion coefficients are approximately constant within each solid solution and are chosen to be equal to the values at the average concentration. The values of D_0, Q, and the interdiffusion coefficients for five selective temperatures in the range of 20 °C to 220 °C are tabulated in Table I. It is seen from Table I that Sn and Cu are the fast diffusing elements in the Cu and Sn matrixes, respectively.

B. *The Interdiffusion Coefficients: $\tilde{D}_\varepsilon$ and $\tilde{D}_\eta$*

To determine the interdiffusion coefficients $\tilde{D}_\varepsilon$ ($=\tilde{D}_2$) and $\tilde{D}_\eta$ ($=\tilde{D}_3$), we require the equilibrium interfacial concentrations, C_{ij}, and the growth constants, k_ε and k_η. The C_{ij} are known from Cu-Sn phase diagram and are listed in Table II. The coefficients k_ε and k_η were measured by Onishi and Fujibuchi[6] over the temperature range of 190 °C to 220 °C and are listed in Table III. The computed values for $\tilde{D}_2$ ($=\tilde{D}_\varepsilon$), $\tilde{D}_3$ ($=\tilde{D}_\eta$), and γ_1, γ_2, and γ_3 (Eq. [6]) are listed in Table IV.

Since the interdiffusion coefficients are sums of terms that have Arrhenius form, they do not, strictly, have Arrhenius form themselves, unless one of the intrinsic diffusivities is negligible. However, the interdiffusion coefficients computed here are well fitted by Arrhenius forms over the temperature range studied. The results are

$$\tilde{D}_2\,(\mathrm{m^2/s}) = \tilde{D}_\varepsilon = 5.48 \times 10^{-9} \exp\left[\frac{-61.86}{RT}\right] \quad [19a]$$

$$\tilde{D}_3\,(\mathrm{m^2/s}) = \tilde{D}_\eta = 1.84 \times 10^{-9} \exp\left[\frac{-53.92}{RT}\right] \quad [19b]$$

where the activation energies are given in kJ/mole.

The interdiffusion coefficients $\tilde{D}_\varepsilon$ and $\tilde{D}_\eta$ were also estimated by Onishi and Fujibuchi,[6] as described in the previous section. Their results were

$$\tilde{D}_2\,(\mathrm{m^2/s}) = D_\varepsilon = 1.43 \times 10^{-8} \exp\left[\frac{-70.6}{RT}\right] \quad [20a]$$

$$\tilde{D}_3\,(\mathrm{m^2/s}) = D_\eta = 1.55 \times 10^{-8} \exp\left[\frac{-64.8}{RT}\right] \quad [20b]$$

Although the pre-exponential constants and activation energies in Eqs. [19] differ from those in Eqs. [20], the differences in D_0 and Q compensate one another; the values of $\tilde{D}_2$ and $\tilde{D}_3$ computed from Eqs. [19] or [20] are in good numerical agreement over the temperature range studied (190 °C to 220 °C). The reason for the difference between the values of D_0 and Q computed here and in Reference 6 is unclear. Reference 6 contains no detailed description of how D_2 and D_3 were found from the concentration profiles; for example, it is not clear what values of D_1 and D_4 were used. The experimental uncertainty in the values of D_1 and D_4 is the principal source of uncertainty in the values of D_0 and Q computed here; the outputs of the calculation from Eqs. [11] through [13] are the ratios, $R_{ij} = D_i/D_j$ (i = 1 through 3, $j = i + 1$), rather than D_i (i = 2 or 3). The values of D_1 and D_4 we used were extrapolated from Reference 36, in which they were measured at temperatures above 350 °C. We know of no more reliable values.

Table III. ε- and η-Phase Growth Data,[6] $W_\varepsilon = k_\varepsilon t^{1/2}$, and $W_\varepsilon = k_\varepsilon t^{1/2}$

Temperature (°C)	k_η (m/s$^{1/2}$)	k_ε (m/s$^{1/2}$)
190	9.39×10^{-9}	5.21×10^{-9}
200	1.06×10^{-8}	6.19×10^{-9}
210	1.19×10^{-8}	7.88×10^{-9}
220	1.43×10^{-8}	8.60×10^{-9}

C. *Interphase Boundary Motion*

The position of the interphase boundaries are determined from Eq. [6] and are fixed by the parameters $\xi_{ij}/\sqrt{t} = 2\gamma_i\sqrt{\tilde{D}_i}$ (i = 1 through 3). The calculated values are listed in Table IV and plotted in Figure 2. The boundary position between the Cu solid solution and the ε phase, ξ_{12}, is negative, which shows that the Cu-ε boundary migrates toward the Cu side. Similarly, the ε-η boundary moves toward Cu. The boundary between the η and Sn moves into the Sn solution but by only about half the distance that ξ_{12} moves into Cu. Therefore, the center of the intermetallic layer (including both ε and η phases) migrates into Cu. These displacements reflect the stoichiometry of the intermetallic phases. Since these are Cu-rich, they consume more Cu than Sn. Unless there is a significant Kirkendall effect, the original Cu-Sn interface is located near the center of the η-phase region and shifts toward the Cu side as the temperature decreases. This result is in general agreement with Reference 6, which reports that diffusion markers placed at the original Cu-Sn interface are found near the center of the η-phase layer after aging. It suggests that the net Kirkendall displacement of the interface is small.

D. *Preferential Growth of η Phase*

As shown in Eqs. [19], the activation energy for interdiffusion in the η phase is lower than that in the ε phase. It follows that the ratio R_{23} ($=\tilde{D}_\varepsilon/\tilde{D}_\eta$) decreases as temperature decreases; R_{23} is equal to 0.37 at 220 °C and reduces to 0.08 at 20 °C. This decrease has the consequence that the η phase fills an increasing fraction of the intermetallic layer as the temperature drops.

Table II. Cu Concentrations (Atom Fraction) at the Interfaces[20]

$C_{1,2}$	$C_{2,1}$	$C_{2,3}$	$C_{3,2}$	$C_{3,4}$	$C_{4,3}$
0.993	0.765	0.755	0.549	0.541	0.00006

Table IV. Calculated Results in This Study and Data in Reference 6

Temperature (°C)	D_2 (m^2/s)	D_3 (m^2/s)	γ_1	γ_2	γ_3
190	5.80×10^{-16}	1.86×10^{-15}	−8648	-9.110×10^{-2}	5.801×10^{-2}
200	7.94×10^{-16}	2.39×10^{-15}	−6130	-8.635×10^{-2}	5.865×10^{-2}
210	1.19×10^{-15}	3.10×10^{-15}	−4555	-7.553×10^{-2}	5.997×10^{-2}
220	1.50×10^{-15}	4.35×10^{-15}	−3336	-8.298×10^{-2}	5.974×10^{-2}

Temperature (°C)	$\frac{\xi_{1/2}}{\sqrt{t}}$ ($m/s^{1/2}$)	$\frac{\xi_{2/3}}{\sqrt{t}}$ ($m/s^{1/2}$)	$\frac{\xi_{3/4}}{\sqrt{t}}$ ($m/s^{1/2}$)	D_2 (m^2/s)[6]	D_3 (m^2/s)[6]
190	-9.60×10^{-9}	-4.39×10^{-9}	5.00×10^{-9}	1.52×10^{-16}	7.54×10^{-16}
200	-1.11×10^{-8}	-4.87×10^{-9}	5.73×10^{-9}	2.24×10^{-16}	1.08×10^{-15}
210	-1.31×10^{-8}	-5.21×10^{-9}	6.68×10^{-9}	3.25×10^{-16}	1.51×10^{-15}
220	-1.50×10^{-8}	-6.43×10^{-9}	7.88×10^{-9}	4.64×10^{-16}	2.10×10^{-15}

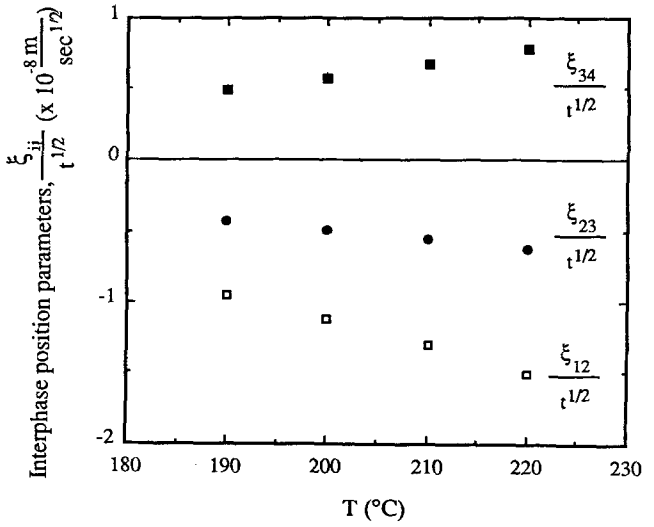

Fig. 2—Calculated interphase position parameters *vs* temperature. ξ_{ij} is the instantaneous position between phase i and j (i, j = 1, Cu solid solution; =2, ε; =3, η; =4, Sn solid solution).

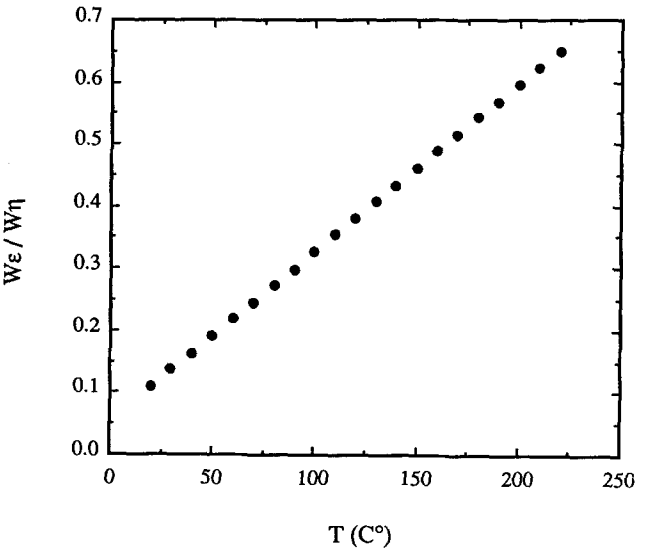

Fig. 3—Calculated ratio of the ε-phase thickness to the η-phase thickness *vs* temperature.

The fraction of η phase was calculated for the case of the Cu-Sn couple. The values of the parameters, γ_i, for the given values of R_{12}, R_{23}, and R_{34} were found from Eqs. [11] through [13]. The ratio of the ε-phase to η-phase width was then calculated from Eqs. [14a] and plotted in Figure 3 as a function of temperature. The ratio decreases almost linearly with temperature, from 0.66 at 220 °C to 0.11 at 20 °C.

While the exact fraction of η phase in the intermetallic layer would differ somewhat for the Cu-solder case ($\tilde{D}_1$ through $\tilde{D}_3$ are the same, but $\tilde{D}_4$ is different), the results should be qualitatively correct for the solder case and are in good agreement with experiment.[5] The fraction of ε phase in the intermetallic layer at the Cu-solder interface increase dramatically as the aging temperature is raised. At temperatures near 20 °C, the ε phase is usually undetectable. Since the overall film thickness is very small at these temperatures and the ε phase should be only ≈10 pct of the film thickness, the high surface-volume ratio of the equilibrium ε phase may well prevent its formation.

E. *Cu- vs Sn-Dominated Growth*

The enhanced growth of the ε phase at high temperature is predominantly due to the higher interdiffusivity in the η phase ($\tilde{D}_\eta > \tilde{D}_\varepsilon$), which is mitigated by a lower activation energy that causes the ratio $R_{23} = \tilde{D}_\varepsilon/\tilde{D}_\eta$ to decrease with temperature. While the intrinsic diffusivities of Cu and Sn in the intermetallic phases cannot be determined by the methods used here, it does not appear necessary to invoke them to understand most of the features of intermetallic growth, including the behavior of inert markers placed at the initial interface.

The limited data on marker migration in Cu-Sn diffusion couples include three pieces of information. First, Reference 14 reports marker motion toward Cu in Cu-Sn diffusion couples at low temperature. Since Sn diffusion in Cu is known to be slower than Cu diffusion in Sn, the markers will naturally migrate toward the Cu interface when the intermetallic thickness is negligible. Second, References 21 and 22 report marker motion toward the Sn-rich side of diffusion couples at high temperature.

However, the couples studied were Cu-bronze (Cu-Sn solid solution) couples. Since the diffusivity of Sn in Cu is larger than the Cu self-diffusivity, this result is expected. Finally, markers in Cu-Sn diffusion couples were reported to migrate toward the Sn side at high temperature.[6] However, it is not clear what reference was used for marker motion. The results of the previous section show that, in the absence of Kirkendall effects, the original Cu-Sn interface is displaced into the intermetallic during diffusion and ultimately appears at about the center of the η phase, near the Sn side of the couple. This prediction is in agreement with the observations reported in Reference 6. While it is extremely unlikely that Cu and Sn have the same intrinsic diffusivities in the intermetallic phases, marker motion toward the Sn-rich side is a natural consequence of intermetallic growth. The stoichiometry of the intermetallic appears to have a more important influence on marker motion than the Kirkendall effect in the intermetallic layer.

V. CONCLUSIONS

A multiphase diffusion model was constructed and used to analyze the growth of the ε- and η-phase intermetallic layers at a plane Cu-Sn interface in a semi-infinite diffusion couple. The model is advantageous with respect to previous ones in that it does not require the assumption or measurement of the precise concentration profiles near the growing interfaces. Experimental measurements of intermetallic layer width as a function of time were used to compute interdiffusivities in the ε and η phases. These were fitted to Arrhenius expressions and used to compute the positions of the interfaces as a function of time.

The results suggest that interdiffusion in the ε phase ($\tilde{D}_\varepsilon$) is well fitted by an Arrhenius expression with $D_0 = 5.48 \times 10^{-9}$ m^2/s and $Q = 61.86$ kJ/mole, while the η-phase interdiffusivity ($\tilde{D}_\eta$) has $D_0 = 1.84 \times 10^{-9}$ m^2/s and $Q = 53.92$ kJ/mole. These results are in reasonable numerical agreement with those of Onishi and Fujibuchi,[6] which were obtained by a different analytic technique.

The interdiffusivity of the η phase is higher than that of the ε phase at all temperatures in the range of 20 °C to 220 °C, which has the consequence that the η phase predominates in the intermetallic layer. However, the lower activation energy for η-phase interdiffusion causes the ratio, $R = \tilde{D}_\eta/\tilde{D}_\varepsilon$, to decrease as temperature rises, with the consequence that the ε phase fills an increasing fraction of the intermetallic layer. At 20 °C, the predicted thickness of the ε phase is ≈10 pct of that of η, while at 200 °C, its thickness is 66 pct of that of η. This effect is governed by the relative values of the interdiffusivity in the intermetallic phases and is not necessarily associated with any change in the relative intrinsic diffusivities of the Cu and Sn species.

Since the intermetallic layer is relatively rich in Cu, it grows predominantly into the Cu phase. If there is no significant Kirkendall effect, the original Cu-Sn interface is located within the η-phase layer after diffusion and lies approximately at the midpoint of the η-phase layer at 220 °C. Hence, the interface appears to shift toward the Sn side of the couple during growth. This prediction is in general agreement with the results of prior work on Cu-Sn diffusion.

LIST OF SYMBOLS

C_i	copper concentration in i phase, $i = 1$ represents copper solid solution phase; $i = 2$, ε phase; $i = 3$, η phase; and $i = 4$, tin solid solution phase
C_{ij}	copper concentration in i phase at the interface between i and j phases
$\tilde{D}_i$	interdiffusion coefficient in i phase, $i = 1$ through 4, representing copper solid solution, ε, η, and tin solid solution phases
D	intrinsic diffusion coefficient
k_ε, k_η	growth constants of ε and η phases, as defined in Eqs. [14a]
ξ_{ij}	position of the interface between i and j phases
γ_i	parameter as defined in Eq. [6]
R_{ij}	$\tilde{D}_i/\tilde{D}_j$
t	time
W	width of intermetallic phase

ACKNOWLEDGMENTS

The authors appreciate the helpful discussions with Dr. George K. Lucey, United States Army, Harry Diamond Laboratories, and Dr. Jin Chan and Mr. David Chu, Lawrence Berkeley Laboratory. This work is supported by the United States Army, Harry Diamond Laboratories, under contract to the Lawrence Berkeley Laboratory.

REFERENCES

1. K.N. Tu: *Acta Metall.*, 1973, vol. 21, pp. 347-54.
2. P.E. Davis, M.E. Warwick, and S.J. Muckett: *Plating Surf. Finishing*, 1983, vol. 70, pp. 49-53.
3. P.E. Davis, M.E. Warwick, and P.J. Kay: *Plating Surf. Finishing*, 1982, vol. 69, pp. 72-76.
4. A.D. Romig, Jr., Y.A. Chang, J.J. Stephens, D.R. Frear, V. Marcotte, and C. Lea: in *Solder Mechanics A State of the Art Assessment*, D.R. Frear, W.B. Jones, and K.R. Kinsman, eds., TMS, Warrendale, PA, 1991, pp. 29-104.
5. A. Sunwoo, J.W. Morris, Jr., and G.K. Lucey, Jr.: *Metall. Trans. A*, in press.
6. M. Onishi and H. Fujibuchi: *Trans. Jpn. Inst. Met.*, 1975, vol. 16, pp. 539-47.
7. L. Revay: *Surf. Technol.*, 1977, vol. 5, pp. 57-63.
8. M.E. Warwick and S.J. Muckett: *Circuit World*, 1983, vol. 9 (5), pp. 5-11.
9. P.J. Kay and C.A. MacKay: *Trans. Inst. Met. Finishing*, 1976, vol. 54, pp. 68-74.
10. U.A. Unsworth and C.A. MacKay: *Trans. Inst. Met. Finishing*, 1973, vol. 51, p. 85.
11. L. Zakraysek: *Weld. J. Res. Suppl.*, 1972, vol. 37 (11), pp. 536-s-41-s.
12. E.K. Ohriner: *Weld. J. Res. Suppl.*, 1987, July, pp. 191-s-202-s.
13. E. Starke and H. Wever: *Z. Metallkd.*, 1964, vol. 55, pp. 107-16.
14. K.N. Tu and R.D. Thompson: *Acta Metall.*, 1981, vol. 30, pp. 947-52.
15. J. Hoyt: *Brazing Soldering*, 1987, no. 13, pp. 10-19.
16. J.O.G. Parent, D.D.L. Chung, and I.M. Bernstein: *J. Mater. Sci.*, 1988, vol. 23, pp. 2564-72.
17. D.S. Dunn, T.F. Marinis, W.M. Sherry, and C.J. Williams: in

Electronics Packaging Materials Science, E.A. Geiss, K.N. Tu, and D.R. Uhlman, eds., MRS, Pittsburgh, PA, 1985, pp. 129-38.
18. A.J. Sunwoo, H. Hayashigatani, J.W. Morris, Jr., and G.K. Lucey, Jr.: *J. Met.*, June 1991, vol. 43 (6), pp. 21-24.
19. Q. Yiyu, F. Hongyuan, C. Dinghua, F. Fuhua, and H. Lixia: *Brazing Soldering*, 1987, no. 13, pp. 39-41.
20. *Binary Alloy Phase Diagrams*, T.B. Massalski, J.L. Murray, L.H. Bennett, and H. Baker, eds., 1987, ASTM, Metals Park, OH, vol. 1, p. 965; M. Hansen: *Constitution of Binary Alloys*, McGraw-Hill Book Company, New York, NY, 1958.
21. H. Oikawa and A. Hosoi: *Scripta Metall.*, 1975, vol. 9, pp. 823-28.
22. K. Hoshino, Y. Iijima, and K. Hirano: *Trans. Jpn. Inst. Met.*, 1980, vol. 21, pp. 674-82.
23. B.F. Dyson, T.R. Anthony, and D. Turnbull: *J. Appl. Phys.*, 1967, vol. 38, p. 3408.
24. B.F. Dyson, T.R. Anthony, and D. Turnbull: *J. Appl. Phys.*, 1966, vol. 37, pp. 2370-74.
25. B.F. Dyson: *J. Appl. Phys.*, 1966, vol. 37, pp. 2375-79.
26. H.B. Huntington, C.-K. Hu, and S.N. Mei: in *Diffusion in Solids: Recent Developments Conf. Proc.*, M.A. Dayananda and G.E. Murch, eds., TMS-AIME, Metals Park, OH, 1984, pp. 97-119.
27. D.R. Dietderich, J. Glazer, C. Lea, W.V. Hassenzahl, and J.W. Morris, Jr.: *IEEE Trans. Magn.*, 1985, vol. MAG-21, pp. 297-300.
28. G.K. Lucey, J. Marshall, C. Handwerker, D. Tench, and A.J. Sunwoo: *Proc. Technique Programs of NEPCON WEST* 1991, vol. 1, pp. 3-10, Feb. 24–28, 1991, Anaheim, CA.
29. L.S. Darken: *Trans. AIME*, 1948, vol. 175, p. 184.
30. W.B. Pearson: *Handbook of Lattice Spacings and Structures of Metals and Alloys*, Pergamon Press, New York, NY, 1958, pp. 125 and 129.
31. P.L. Brooks and E. Gillam: *Acta Metall.*, 1970, vol. 18, pp. 1181-85.
32. A. Gangulee, G.C. Das, and M.B. Bever: *Metall. Trans.*, 1973, vol. 4, pp. 2063-66.
33. W. Jost: *Diffusion in Solids, Liquids, and Gases*, 2nd ed., Academic Press, New York, NY, 1960, p. 68.
34. J.S. Kirkaldy: *Can. J. Phys.*, 1958, vol. 36, p. 917.
35. *Handbook of Mathematics*, People's Education Press, Beijing, 1979, p. 106.
36. W. Seith and T. Heumann: *Diffusion of Metals: Exchange Reactions*, United States Atomic Energy Commission, 1962, translated from a publication of Springer Press, Berlin, pp. 65 and 68.
37. T. Heumann: *Z. Phys. Chem.*, 1952, vol. 201, p. 168; also in W. Seith and T. Heumann, *Diffusion of Metals: Exchange Reactions*, United States Atomic Energy Commission, 1962, translated from a publication of Springer Press, Berlin, pp. 150-54.